materials proceedings

MDPI

Proceeding Paper

Characterization and Comparison of WO_3 with Hybrid WO_3-MoO_3 and TiO_2 with Hybrid TiO_2-ZnO Nanostructures as Photoanodes †

M. Cifre-Herrando, G.-Roselló-Márquez, P. J. Navarro-Gázquez, M. J. Muñoz-Portero, E. Blasco-Tamarit and J. García-Antón *

Ingeniería Electroquímica y Corrosión (IEC), Instituto Universitario de Seguridad Industrial, Radiofísica y Medioambiental (ISIRYM), Universitat Politècnica de València, C/Camino de Vera s/n, 46022 Valencia, Spain; email1@gmail.com (M.C.-H.); email2@gmail.com (G.-R.-M.); email3@gmail.com (P.J.N.-G.); email4@gmail.com (M.J.M.-P.); email5@gmail.com (E.B.-T.);

* Correspondence: jgarciaa@iqn.upv.es

† Presented at the 4th International Online Conference on Nanomaterials, 5–19 May 2023; Available online: https://iocn2023.sciforum.net.

Abstract: Tungsten oxide (WO_3) and zinc oxide (ZnO) are n-type semiconductor with numerous applications in photocatalysis. The objective of this study was to synthesize and characterize different types of nanostructures (WO_3, WO_3-Mo, TiO_2 and TiO_2-ZnO) for a comparison of hybrid and pure nanostructures to use them as a photoanodes for hydrogen production. With the aim of comparing the properties of both samples, Field Emission Scanning Electron Microscopy (FE-SEM) and Confocal Laser-Raman Spectroscopy have been used to study the morphology and composition and crystallinity, respectively. Finally, water splitting measurements were performed to compare the photoelectrochemical properties of the photoanodes.

Keywords: nanostructures; hybrid nanostructures; WO_3; TiO_2; water splitting; emerging contaminants

Citation: Cifre-Herrando, M.; G.-Roselló-Márquez; Navarro-Gázquez, P.J.; Muñoz-Portero, M.J.; Blasco-Tamarit, E.; García-Antón, J. Characterization and Comparison of WO_3 with Hybrid WO_3-MoO_3 and TiO_2 with Hybrid TiO_2-ZnO Nanostructures as Photoanodes. *Mater. Proc.* **2023**, *14*, x. https://doi.org/10.3390/xxxxx

Published: 5 May 2023

1. Introduction

The high severity of environmental problems caused by the increase of CO_2 in the atmosphere has increased the scientific research into new and renewable energy sources. Hydrogen is considered one of the most promising energy sources to replace fossils fuels. Photoelectrochemical (PEC) water splitting using solar light is a novel method to produce clean and sustainable hydrogen from water and sunlight. For an efficient PEC process, it is necessary to find a suitable semiconductor photoelectrode. Oxide semiconductors are the most common materials, in particular, those with a high visible-light absorption, efficient charge carrier separation and chemical stability, which could be TiO_2 or WO_3 [1].

On one hand, WO_3 is claimed to be a proper material for PEC water splitting application due to its high resistance to photocorrosion, stability in acidic media, good electron transport properties and its band gap (Eg = 2.6-eV). As its band gaps is capable of only capturing 12% of the incident light of the solar spectrum, several approaches have been tried to enhance PEC of WO_3 by band-gap modifications [2]. Doping of WO_3 with Mo can narrow the band gap of WO_3 and consequently, improve the photocatalytic properties [3]. Therefore, a simple method for the synthesis of hybrid WO_3-MoO_3 nanostructures is proposed.

On the other hand, TiO_2 is one of the most extensively studied material for PEC [4]. This is because it is a non-toxic semiconductor, has high chemical stability, excellent photocatalytic activity, cost effectiveness, and capacity to generate electron/hole pairs [5].

However, its photocatalytic applications is limited to ultraviolet irradiation due to its wide value of bandgap (3.2 eV) [6]. In order to reduce its bandgap, different elements could be added to TiO_2 nanostructures. In this study, hybrid nanostructures of TiO_2 with ZnO are synthesized to increase the TiO_2 efficiency in water splitting PEC.

Thus, the objective of this work is to synthesize and characterize different types of nanostructures (WO_3, hybrid WO_3-MoO_3, TiO_2 and TiO_2-ZnO) for a comparison of hybrid and pure nanostructures. Then, they will be used as a photoanodes for PEC water splitting to produce hydrogen.

2. Materials and Methods

2.1. Synthesis of Nanostructures

The procedure to synthesize nanostructures was conducted by electrochemical anodization under hydrodynamic conditions using a rotatory disk electrode. The process was optimized by the authors in previous works [7,8].

For the WO_3 nanostructures, anodization of W was carried out at a velocity of 375 rpm, applying 20 V for 4 h. The electrolyte consisted of 1.5 M methanosulfonic acid and 0.01 M citric acid at 50 °C. The tungsten bar was placed on a rotating disk electrode, and it was rotated at a speed of 375 rpm. After anodization, WO_3 nanostructures were annealed at 600 °C in an air atmosphere for 4 h.

For synthesizing hybrid nanostructures of WO_3-MoO_3, the same anodization was carried out but different concentrations of $Na_2MoO_4{\cdot}2H_2O$ (Mob) were added to the electrolyte.

For the TiO_2, the electrochemical anodization of Ti was carried out at room temperature under 3000 rpm applying 30 V during 3 h in a glycerol/water (60:40 vol %) electrolyte with a concentration of 0.27 M NH_4F. Finally, the samples were annealed at 450 °C for 1 h in air atmosphere to transform TiO_2 nanostructures to the anatase phase.

For the TiO_2-ZnO hybrid nanostructures, after forming TiO_2 nanosponges, the ZnO electrodeposition process was performed from a $Zn(NO_3)_2$ solution at 75 °C using a potential of −0.86 $V_{Ag/AgCl}$ for 15 min in an Autolab PGSTAT302N potentiostat. A three-electrode electrochemical cell was used, where TiO_2 nanosponges were used as working electrode, an Ag/AgCl (3 M KCl) electrode was used as reference electrode, and a platinum tip was used as counter electrode. The influence of $Zn(NO_3)_2$ concentration (1–10 mM was studied to analyse how affects the photoelectrochemical activity of the photoelectrodes

2.2. Morphological and Crystalline Characterization

The morphology of the samples was characterized using Field Emission Scaning Electron Microscopy (FE-SEM) with Energy-Dispersive X-ray spectroscopy (EDX), which was used to identify the elements that formed the nanostructures. The equipment used was a Zeiss Ultra-55 Scanning Electron Microscope applying 20 kV. In addition, the crystallinity of the samples was analysed using a Raman Confocal Laser Spectroscopy (Witec alpha300R) with a neon laser (488 nm) and a power of 420 μW.

2.3. Photoelectrochemical Properties—Water Splitting Tests

Photoelectrochemical experiments were performed using an Autolab PGSTAT302N potentiostat and a solar simulator (AM 1.5, 100 $mW{\cdot}cm^{-2}$). A three-electrode cell configuration was used, consisting of an Ag/AgCl (3 M KCl) reference electrode, a platinum tip as a counter electrode, and the nanostructures as a working electrode. A potential sweep was performed with a scan rate of 2 $mV{\cdot}s^{-1}$ by chopped light irradiation (60 mV (30 s) in the dark and 20 mV (10 s) with light).

3. Results and Discussion

3.1. FE-SEM

Figure 1 shows the FE-SEM images of the synthesized nanostructures. Observing the images of Figure 1a,b the effect of doping the WO_3 nanostructures with MoO_3 can be observed. In both cases, defined small-sized nanoparticles with a mountain-shape were obtained. In contrast, Figure 1c,d allows to compare the effect of adding ZnO into the TiO_2 nanostructures. Figure 1c shows nanostructures with a rough surface and high specific area, typical from a nanosponge-like morphology [9]. Figure 1d shows the general appearance of the hybrid nanostructures TiO_2-ZnO, where it can be also observed a nanosponge-shaped nanostructure without the presence of anomalous particles on its surface. Consequently, the morphology is the same for the pure nanostructure than for the hybrid. This indicates that no MoO_3 or ZnO agglomerations occurred during the doping process [5].

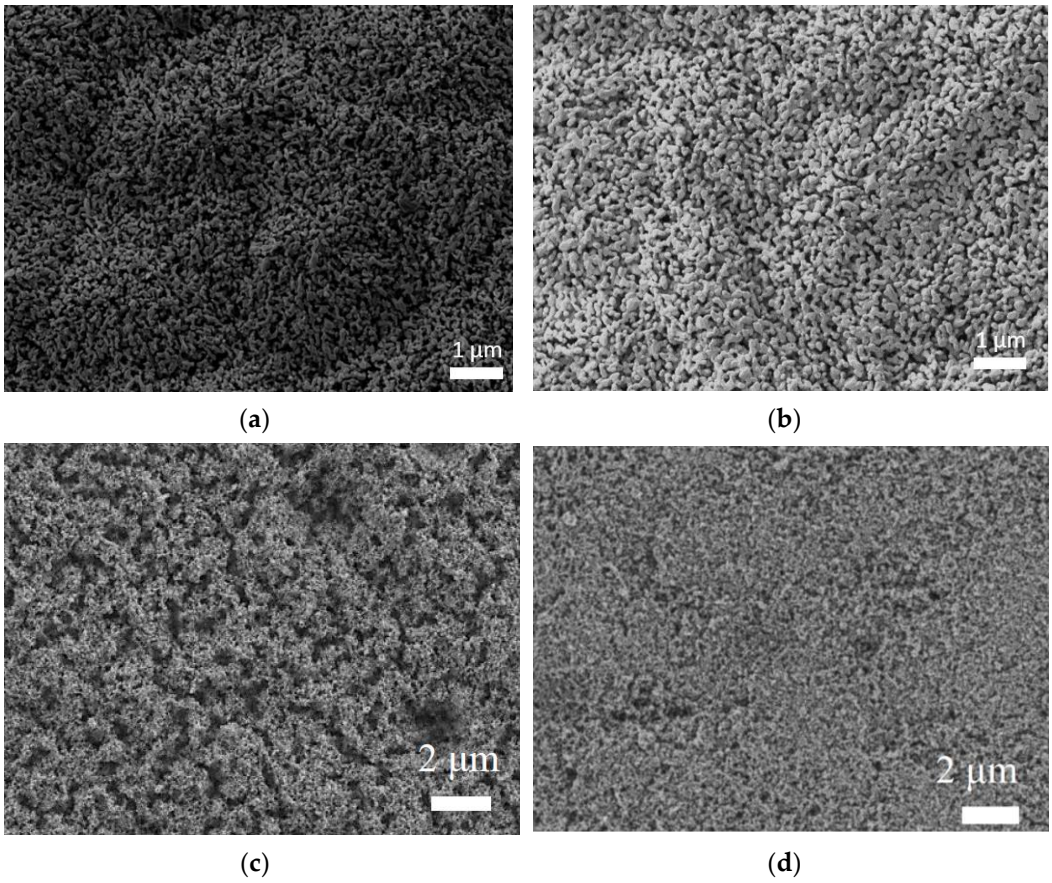

(**a**) (**b**)

(**c**) (**d**)

Figure 1. FE-SEM images of the different nanostructures (**a**) WO_3 (**b**) WO_3 + 0.01 M Mob (**c**) TiO_2 and (**d**) TiO_2 + 0.01 M ZnO.

EDX analysis has been carried out to prove the presence of MoO_3 and ZnO in the nanostructures and to quantify the elements. Table 1 shows the results of the EDX analysis for both hybrid nanostructures. In the case of MoO_3 addition, the percentage of MoO_3 increases when increasing the concentration in the electrolyte. Similarly, for the ZnO deposition, the quantity of Zn in the samples increases by increasing the concentration of ZnO in the electrodeposition. Consequently, it can be affirmed that MoO_3 and ZnO are deposited over the pure nanostructure.

Table 1. Results of the EDX analysis shown as percentage, in weight and atomic, for the different elements present in the samples.

Concentration of Mob (M)	% (Weight)			% (Atomic)			Concentration of $Zn(NO_3)_2$ (M)	% Weight			% Atomic		
	O	W	M	O	W	M		O	Ti	Zn	O	Ti	Zn
0	18.02	81.98	0.00	71.66	28.33	0.00	**0**	34.51	65.49	0.00	61.21	38.79	0.00
0.001	28.77	70.32	0.92	82.10	17.46	0.44	**0.001 M**	38.11	57.56	4.33	65.26	32.92	1.82
0.005	19.40	78.88	1.71	73.07	25.85	1.08	**0.005 M**	36.07	58.08	5.85	63.39	34.10	2.51
0.01	18.01	80.02	1.97	71.18	27.53	1.30	**0.01 M**	35.04	57.81	7.15	62.45	34.43	3.12

3.2. Raman

The Raman spectra of the different nanostructures are presented in Figure 2. Figure 2a shows the Raman spectra of the WO_3 nanostructure and the hybrid WO_3-MoO_3 nanostructures after a heat treatment of 600 °C for 4 h, where it can be appreciated the peaks located at 135, 270, 714, 805 and 955 cm^{-1}, which are those corresponding to monoclinic WO_3. As seen in the spectra, the relative intensity of the bands diminishes as increasing the percentage of Mob in the electrolyte. In addition, the Raman spectra show the principal bands of MoO_3: 190, 647, 867 955 cm^{-1} [10]. Figure 2b shows the spectra of the TiO_2 nanostructures after a heat treatment of 450 °C for 1 h. For the pure nanostructure, the peaks associated with the anatase phase of TiO_2 are observed (145, 397, 520 and 635 cm^{-1}). However, for the hybrid nanostructure with ZnO, the peaks are not observed due to the high fluorescence of ZnO. Therefore, this allows us to reaffirm that ZnO is indeed deposited on the TiO_2 nanostructure.

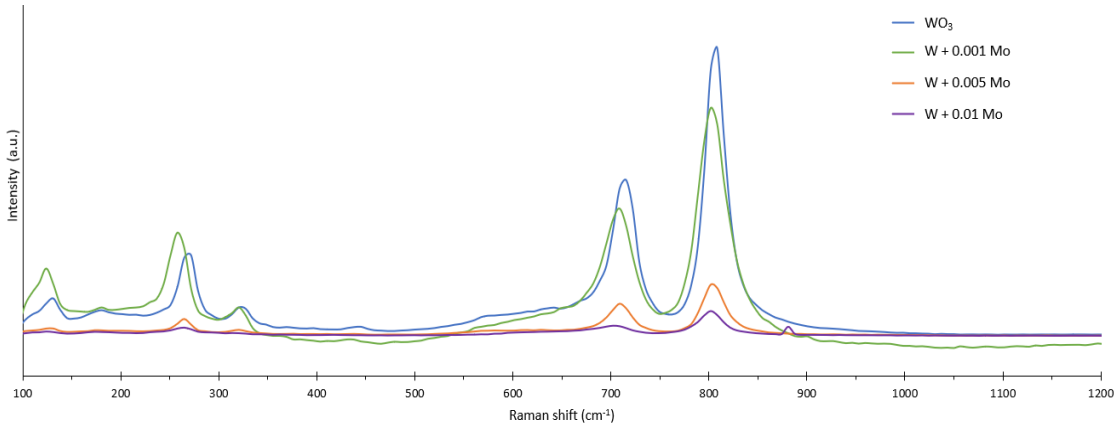

(**a**)

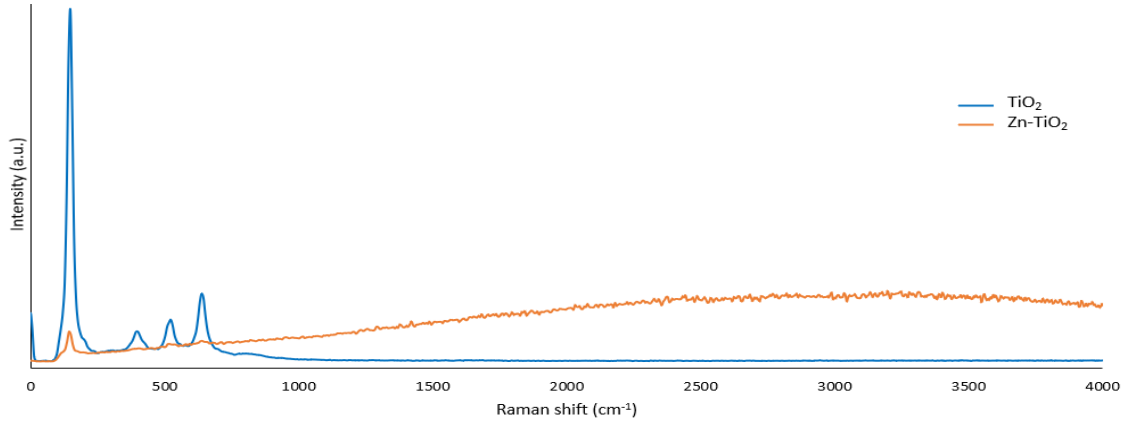

(**b**)

Figure 2. Raman spectra of the nanostructures (**a**) WO_3 + different Mob concentrations (**b**) TiO_2 and TiO_2 + ZnO.

3.3. Water Splitting Tests

The influence of the doping element concentration in the electrolyte on the photoelectrochemical (PEC) behavior of the nanostructures was also tested by water splitting tests, shown in Figure 3. For Mob, it can be seen from Figure 3a, that the sample with higher photoresponse is that one without Mob. Furthermore, as the concentration of Mob increases the photocurrent decreases, indicating worse photoelectrochemical properties. The worsening of the nanostructure after the addition of MoO_3 could be explained by the fact that MoO_3 is deposited on the surface of the nanostructure and prevents electron transfer.

On the other hand, from Figure 3b it can be seen that the sample with higher photocurrent is that one with 0.01 M ZnO. Furthermore, by increasing the ZnO concentration, the photoelectrochemical performance of the nanostructures improves. This is ought to the fact that ZnO crystals increases the photocatalytic activity of the nanostructures and the useful life of the excited electrons, reducing recombination processes.

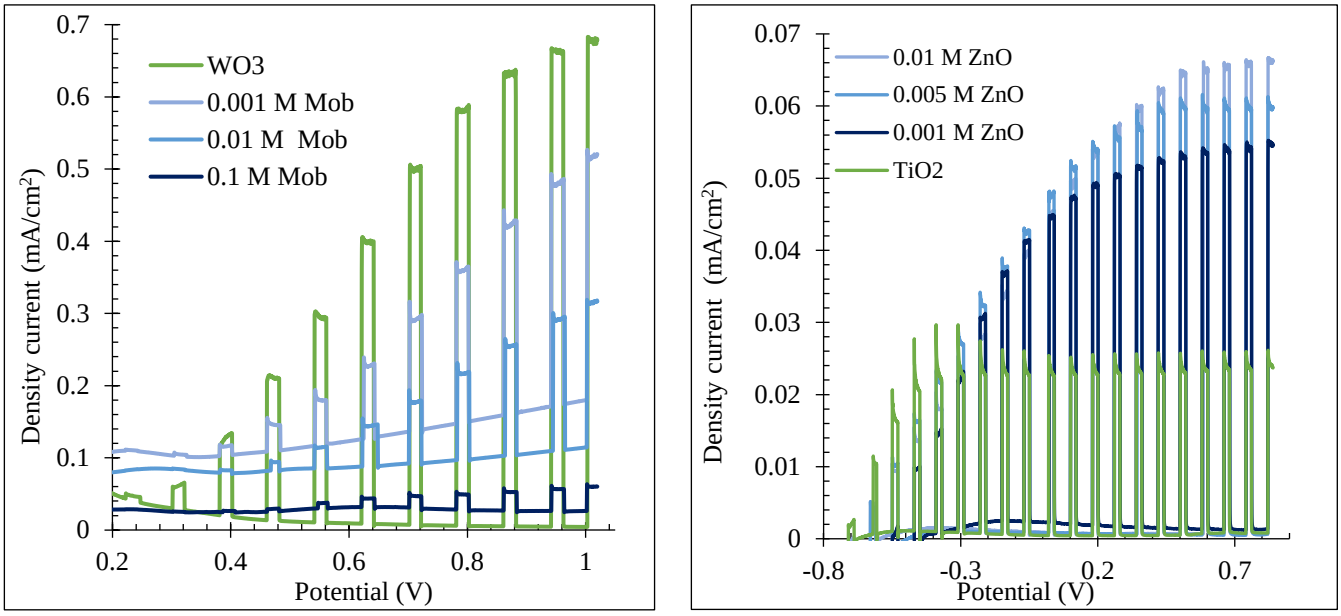

(**a**) (**b**)

Figure 3. Water splitting curves of the (**a**) WO_3 nanostructures synthesized with different Mob concentrations and (**b**) TiO_2 nanostructures synthesized with different ZnO concentrations.

4. Conclusions

In this research, different types of nanostructures (WO_3 and TiO_2) have been synthesized by anodization of W and Ti, respectively, under hydrodynamic conditions. Next, hybrid nanostructures have been also synthesized with WO_3-MoO_3 and TiO_2-ZnO to improve the original nanostructures. For the case of WO_3-MoO_3, the photocatalytic activity of the nanostructures could not be increased by electrodeposition of MoO_3 in the surface of the WO_3 nanostructures. In contrast, the photocatalytic activity of the TiO_2-ZnO was significantly enhanced compared to TiO_2 nanosponges. The optimum nanostructure was achieved when performing the ZnO electrodeposition with a 0.01 M $Zn(NO_3)_2$ concentration, obtaining a photoelectrochemical response 141% higher compared to the crystalline TiO_2 nanosponges.

Author Contributions: Conceptualization, M.C.-H. and G.-R.-M.; methodology, M.C.-H., P.J.N.-G. and G.-R.-M.; investigation, M.C.-H., P.J.N.-G.; resources, G.-R.-M.; writing M.C.-H. and G.-R.-M.; supervision, E.B.-T., M.J.M.-P., J.G.-A. All authors have read and agreed to the published version of the manuscript.

Acknowledgments: Authors would like to express their gratitude to AEI (PID2019-105844RB-I00/AEI/10.13039/501100011033) for the financial support. M. Cifre-Herrando thanks Ministerio de Universidades for the concession of the pre-doctoral grant (FPU19/02466). G. Roselló-Márquez thanks the UPV for the concession of a post-doctoral grant (PAID-10-21). P.J. Navarro-Gázquez also thanks the Grant PEJ2018-003596-A-AR funded by MCIN/AEI/10.13039/501100011033. Finally, project co-funded by FEDER operational programme 2014-2020 of Comunitat Valenciana (IDIFEDER/18/044) is acknowledged.

Conflicts of Interest: "The authors declare no conflict of interest.".

References

1. Becker, J.-P.; Urbain, F.; Smirnov, V.; Rau, U.; Ziegler, J.; Kaiser, B.; Jaegermann, W.; Finger, F. Modeling and Practical Realization of Thin Film Silicon-Based Integrated Solar Water Splitting Devices. *Phys. Status Solidi* **2016**, *213*, 1738–1746. https://doi.org/10.1002/pssa.201533025.
2. Liu, X.; Wang, F.; Wang, Q. Nanostructure-Based WO_3 Photoanodes for Photoelectrochemical Water Splitting. *Phys. Chem. Chem. Phys.* **2012**, *14*, 7894–7911. https://doi.org/10.1039/C2CP40976C.
3. Li, N.; Teng, H.; Zhang, L.; Zhou, J.; Liu, M. Synthesis of Mo-Doped WO_3 Nanosheets with Enhanced Visible-Light-Driven Photocatalytic Properties. *RSC Adv.* **2015**, *5*, 95394–95400. https://doi.org/10.1039/c5ra17098b.
4. Harris, J.; Silk, R.; Smith, M.; Dong, Y.; Chen, W.-T.; Waterhouse, G.I.N. Hierarchical TiO2 Nanoflower Photocatalysts with Remarkable Activity for Aqueous Methylene Blue Photo-Oxidation. *ACS Omega* **2020**, *5*, 18919–18934. https://doi.org/10.1021/acsomega.0c02142.
5. Navarro-Gazquez, P.J.; Muñoz-Portero, M.J.; Blasco-Tamarit, E.; Sánchez-Tovar, R.; Fernández-Domene, R.M.; García-Antón, J. Original Approach to Synthesize TiO_2/ZnO Hybrid Nanosponges Used as Photoanodes for Photoelectrochemical Applications. *Materials* **2021**, *14*, 6441.
6. Mor, G.K.; Varghese, O.K.; Paulose, M.; Shankar, K.; Grimes, C.A. A Review on Highly Ordered, Vertically Oriented TiO2 Nanotube Arrays: Fabrication, Material Properties, and Solar Energy Applications. *Sol. Energy Mater. Sol. Cells* **2006**, *90*, 2011–2075. https://doi.org/10.1016/j.solmat.2006.04.007.
7. Cifre-Herrando, M.; Roselló-Márquez, G.; García-García, D.M.; García-Antón, J. Degradation of Methylparaben Using Optimal WO_3 Nanostructures: Influence of the Annealing Conditions and Complexing Agent. *Nanomaterials* **2022**, *12*, 4286. https://doi.org/10.3390/nano12234286.
8. Fernández-Domene, R.M.; Sánchez-Tovar, R.; Sánchez-González, S.; Garcia-Anton, J. Photoelectrochemical Characterization of Anatase-Rutile Mixed TiO_2 Nanosponges. *Int. J. Hydrog. Energy* **2016**, *41*, 18380–18388.
9. Borràs-Ferrís, J.; Sánchez-Tovar, R.; Blasco-Tamarit, E.; Fernández-Domene, R.M.; Garcia-Anton, J. Effect of Reynolds Number and Lithium Cation Insertion on Titanium Anodization. *Electrochim. Acta* **2016**, *196*, 24–32.
10. Jittiarporn, P.; Sikong, L.; Kooptarnond, K.; Taweepreda, W.; Stoenescu, S.; Badilescu, S.; Truong, V. Van Electrochromic Properties of MoO_3-WO_3 Thin Films Prepared by a Sol-Gel Method, in the Presence of a Triblock Copolymer Template. *Surf. Coat. Technol.* **2017**, *327*, 66–74. https://doi.org/10.1016/j.surfcoat.2017.08.012.